Molecular-dynamics simulation of growth of nanocrystals in an amorphous matrix

J. K. Bording* and J. Taftø

Department of Physics, University of Oslo, P.O. Box 1048, Blindern, 0316 Oslo, Norway
(Received 9 December 1999; revised manuscript received 17 May 2000)

Using germanium as an example we study the growth of crystalline nuclei by molecular dynamics. Starting with crystalline nuclei of different sizes embedded in an amorphous matrix we follow the evolution of the system at the atomic level. At a temperature about halfway between absolute zero and the melting temperature, we observe that crystallites of diameter larger than 2.0 nm grow, while smaller crystals disappear.

I. INTRODUCTION

Classical theory of nucleation and growth of crystallites in a supercooled or amorphous matrix relies on the concept of surface tension, or Gibbs free energy to be more precise. The interface is, in this phenomenological theory, a mathematical concept that is not easily accessible for experimental observations. Contrary to the interface energy between a liquid and a smooth surface of a bulk solid, it is extremely difficult to measure the interface free energy between a crystalline nucleus and an amorphous matrix. Furthermore, while the atomic arrangement at a planar interface between two solid phases can be studied in great detail with a state-of-the-art high-resolution transmission electron microscope, this challenge awaits realization for the curved interface around a small nucleus. The dynamic nature, in addition to complicated geometry, not only calls for high spatial resolution and sensitivity, but also for high temporal resolution.

Nucleation and growth can be addressed by molecular-dynamics simulations using powerful computers. Several investigators have used the simple Lennard-Jones pair potential to study nucleation and growth.[1–3] In order to simulate most systems accurately, more elaborate potentials involving many-body interactions are needed. For the semiconductors silicon and germanium, accurate interatomic potentials are available in the literature.[4–6] One of these, the Stillinger and Weber potential,[6] has previously been used to study the kinetics of dissolution of silicon crystals.[7] We use the potential of Tersoff[4,5] and study the early stage of crystallization of germanium at high supercooling. The reason for choosing germanium as the material to simulate is that we[8] have already shown by molecular-dynamics simulation with the Tersoff potential that the simulated structure of amorphous germanium is in excellent agreement with high-quality diffraction experiments.[9] A penalty for using this accurate, but unfortunately rather complex potential is the increasing computation time. Thus even with the most powerful computers we are able to scan only a very small volume in space-time, making it extremely unlikely to observe the creation of a nucleus that grows to the critical size. We circumvent this problem by embedding crystallites of different sizes in the amorphous matrix and study their development with time. For crystallites smaller than the critical size we mostly observe annihilation, which is the time reversal of the "fluctuation" causing the creation of a nucleus.

After a brief introduction to classical theory of nucleation we will in this paper present details about the molecular-dynamics simulations we have undertaken. We calculate the spatial variations in energy, and we present results for the local structure of the crystalline/amorphous boundary as well as the evolution of the embedded nuclei.

Classical nucleation theory

We will now briefly review the classical theory of nucleation that we later will use to put the result of our simulations into perspective. According to this theory the additional free energy related to the formation of a crystalline nucleus with radius r in an amorphous matrix can be written as

$$\Delta G_{total} = \frac{4}{3}\pi r^3 \Delta G_{phase} + 4\pi r^2 \gamma. \tag{1}$$

Here ΔG_{phase} is the difference in free energy between the nucleus phase and the matrix phase. This is a driving force for crystallization when the crystalline nucleus phase has lower free energy than the amorphous matrix phase. γ is the surface tension, or additional free energy per unit area associated with the boundary between the two different phases. This energy is positive and will act as a barrier to the formation and growth of the nucleus. If ΔG_{phase} is negative we see from Eq. (1) that there exists a critical size

$$r^* = \frac{-2\gamma}{\Delta G_{phase}}. \tag{2}$$

For nuclei smaller than r^*, a reduction in size will also give a reduction in the total free energy. Such nuclei, often called embryos, will reduce in size and vanish. However, for nuclei larger than r^*, the size must increase to reduce the total free energy. r^* cannot often, however, be calculated from Eq. (2) because of the difficulty of obtaining reliable values for γ.

II. SIMULATION PROCEDURE

The amorphous phase prior to the insertion of the nuclei was a cubic simulation cell with 4096 atoms and periodic boundary conditions. Its structure was a typical continuous random network, with a radial distribution function in very good agreement with diffraction experiments on amorphous germanium.[9] Details about the preparation and structure of the amorphous material were reported in a previous paper.[8]

Spherical crystalline nuclei were embedded in this matrix by replacing the atoms inside a sphere in the center of the simulation cell with a perfect spherical crystal with the diamond structure. Prior to insertion, both the amorphous matrix and the crystal were heated to 2000 K* at zero external pressure using molecular dynamics. Notice the asterisk on the temperature unit. We use this symbol to distinguish the simulation temperature scale from the Kelvin scale (see Ref. 8 for further details). This is done because germanium simulated with the Tersoff[4,5] potential has a melting temperature of 3200 K*, much higher than real germanium.

We made 15 simulation cells with varying nuclei size. Because of the varying nuclei size and local density in the amorphous matrix, the number of atoms in the inserted spherical crystallite was not necessarily exactly the same as the number of atoms taken out. Thus the new simulation cell contained a total number of atoms that could deviate slightly from the original 4096. The cubic computation cells had sides of about 4.5 nm, large enough to prohibit the crystalline nucleus to interact with itself.

The insertion of the spherical crystal produced an interface with many unfortunate configurations and thus a high internal potential energy. This energy was initially removed by relaxing the system with a steepest-descent method into the nearest local energy minimum. This was done to avoid the sudden release of large amounts of energy, which would cause the entire system to melt. The new simulation cells, with an amorphous matrix and a crystalline nucleus, were then simulated at 2000 K* with zero external pressure in a molecular-dynamics simulation. This is above $\frac{1}{2}T_m$, where T_m is about 3200 K* using the Tersoff potential, so the atoms have significant mobility. At the same time, the temperature is low enough to give a critical size so small that it can be probed in a simulation. The systems were initially kept at this temperature and pressure for 5000 time steps in order to reach steady state, and then another 350 000 time steps to study the evolution of the nuclei. A simulation like this, at this temperature, is effectively an annealing. Each time step is 2.0×10^{-15} s, giving a total simulation time for each of the configurations of 0.7 ns. All simulations were done with constant number of atoms, pressure, and temperature (NPT) using the velocity Verlet algorithm.

As for most analytical potentials, the Tersoff potential[4,5] calculates the potential energy of an ensemble of atoms as a sum over N individual single atomic energies:

$$\Phi = \sum_{i=1}^{N} \phi_i. \tag{3}$$

Although it is only the total potential energy that is a well-defined quantity, we will in this paper utilize the single atomic energies, ϕ_i. By doing so we are able to map the energy with large spatial resolution that is particularly interesting in the boundary region between the amorphous and crystalline phases. Notice that in order to obtain the *total* internal energy, the kinetic energy for the ensemble of atoms must be added ($\Sigma_{i=1}^{N} \frac{1}{2} m_i v_i^2$). This provides, however, no new information in our simulations.
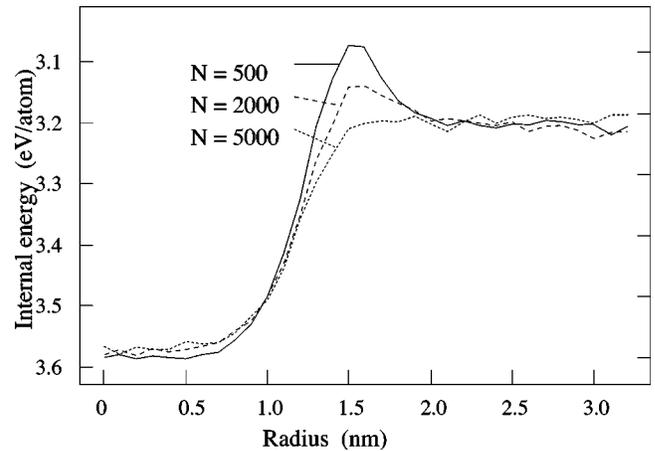

FIG. 1. Energy profile at 500, 2000, and 5000 time steps. The radius of the inserted crystalline nucleus in this case is 1.5 nm, and the system was kept at 2000 K*.

III. RESULTS

A. Internal energy across the interface

In Fig. 1 we have plotted the energy profile at three different times at the initial stage of the simulation. With the energy profile we mean the average single atomic energy ϕ_i as a function of the distance from the center of the nucleus. The insertion of the spherical crystal resulted in atoms in the boundary region with very unfavorable configurations, and thus high energy. After the steepest-descent relaxation most of this energy was removed, but the atoms still had an elevated energy compared to the adjacent bulk phases. This is seen by the peak, or barrier, in the energy profile of Fig. 1 right at the position of the original boundary. After some annealing at 2000 K* the barrier reduced its height, and eventually after about 5000 time steps, or 10 ps, it was completely removed. Although the peak did not last very long, it lasted long enough to indicate that the rearrangement in the boundary region was more than just a minute movement of some of the atoms. The rearrangement in the crystalline phase was rather gradual, while in the amorphous phase it was more varying. Some atoms moved as far as 0.1 nm, while others were nearly stationary.

Notice from Fig. 1 that the potential energy of both the crystalline and the amorphous phase away from the boundary is constant and equals the energy of the respective bulk phases. The barrier close to the boundary vanished after about 5000 time steps, and thus there is no indication of a barrier in the internal energy. However, the barrier may still be present in the free energy. In order to obtain the free energy we need to know the entropy.

B. Atomic order across the interface

In principle, the entropy can be extracted from molecular dynamics simulations, and Ma,[10] for instance, has proposed a procedure to do so. However, in practice this is a very time-consuming procedure, where an enormous number of states has to be probed. Lacking a better alternative, we consider the crystalline order across the interface to assess the entropy as a function of the distance from the center of the nuclei.
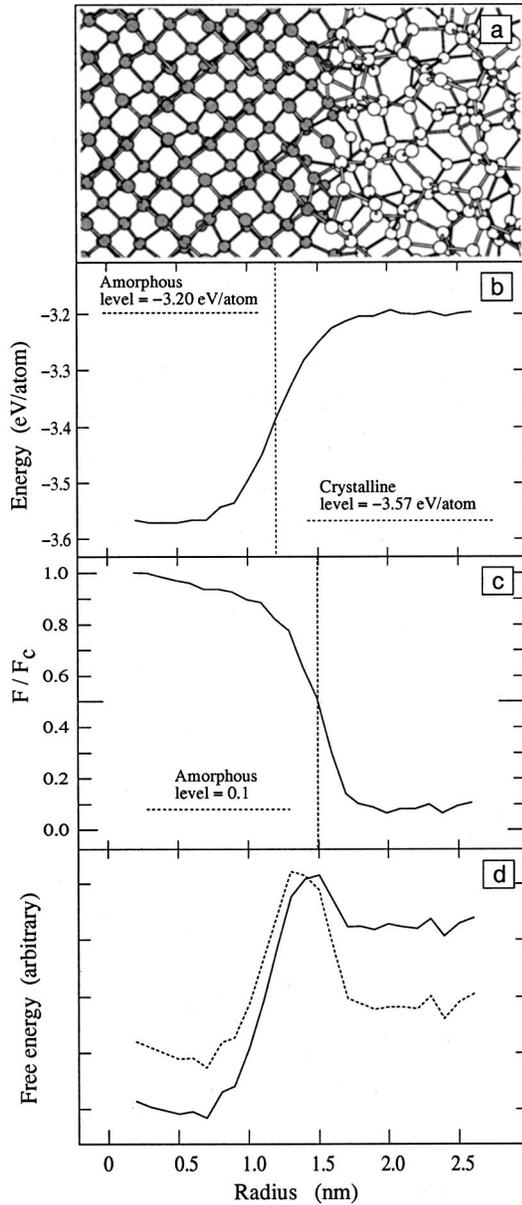
FIG. 2. A snap shot of a typical boundary between a spherical crystal of 3 nm and the amorphous matrix (a). (b) and (c) are internal potential energy and order profiles, respectively, across this boundary. The vertical lines in (b) and (c) indicate the position of the intermediate value of the internal energy and normalized structure factor, respectively. We chose the vertical line in (c) as the boundary position. The temperature of the system was 2000 K*. (d) is, as explained in the text, an estimate for the free energy across the boundary at two arbitrary temperatures.

More precisely, we calculate the average structure factor from the atoms lying in a shell, of thickness 0.1 nm, around the center of the nuclei:

$$F(\mathbf{g}, \mathbf{R}) = \frac{1}{N_R} \left| \sum_{j=1}^{N_R} e^{2\pi i \mathbf{g} \cdot \mathbf{r}_j} \right|, \qquad (4)$$

where $\mathbf{R}$ is the radius of the shell, $\mathbf{r}_j$ is the position of atom j, N_R is the number of atoms in the shell, and $\mathbf{g}$ is the reciprocal [111] vector. Other choices for $\mathbf{g}$ were tested, but no important difference was found.
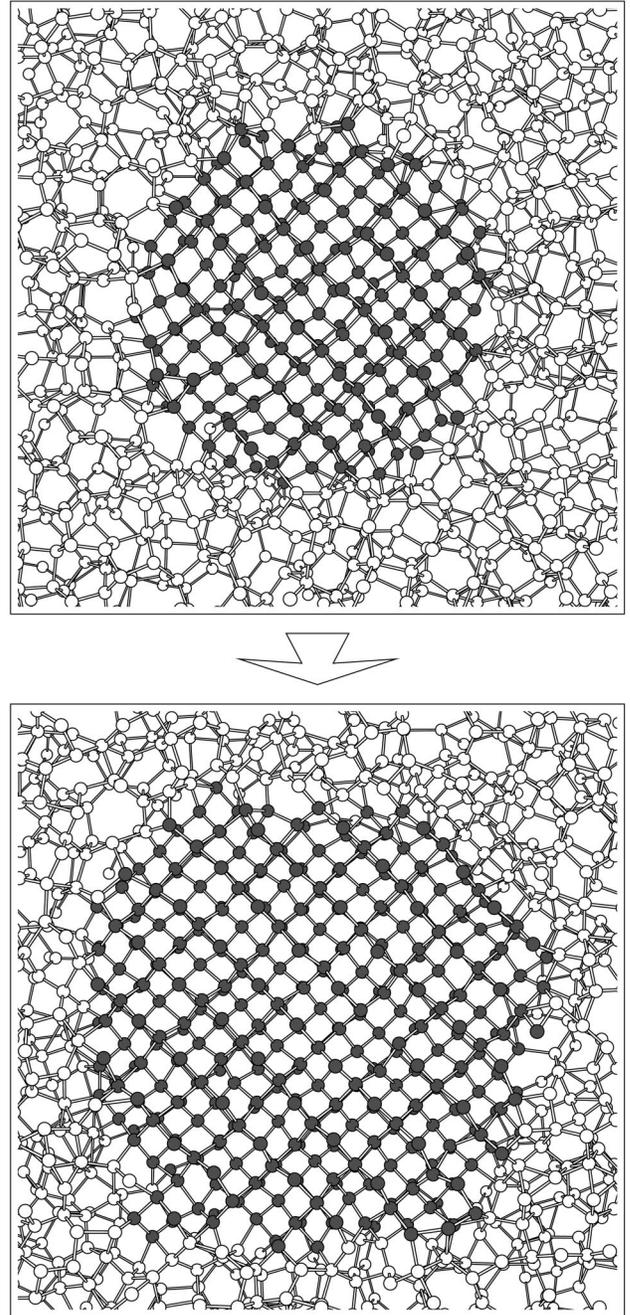

FIG. 3. Snapshots of an embedded nucleus *larger* than the critical size, at 2000 K*. The time interval between the snapshots are 0.5 ns. The size of the squares are 4.5 nm×4.5 nm.

The normalized structure factor is plotted in Fig. 2(c). The normalization is done by dividing the structure factor from the shell of simulated atoms, $F(\mathbf{R})$, with the structure factor from a shell of perfect crystal, $F_c(\mathbf{R})$, at the same temperature. Thus, for a shell of perfect crystal the normalized structure factor is unity. Due to strain this does not happen close to the interface. For crystals smaller than about 2.0 nm, however, we see from Fig. 2(c) that the entire crystal will to some degree be deformed. If the matrix were polycrystalline rather than a continuous random network, the stress could probably be larger, deforming even larger crystals.
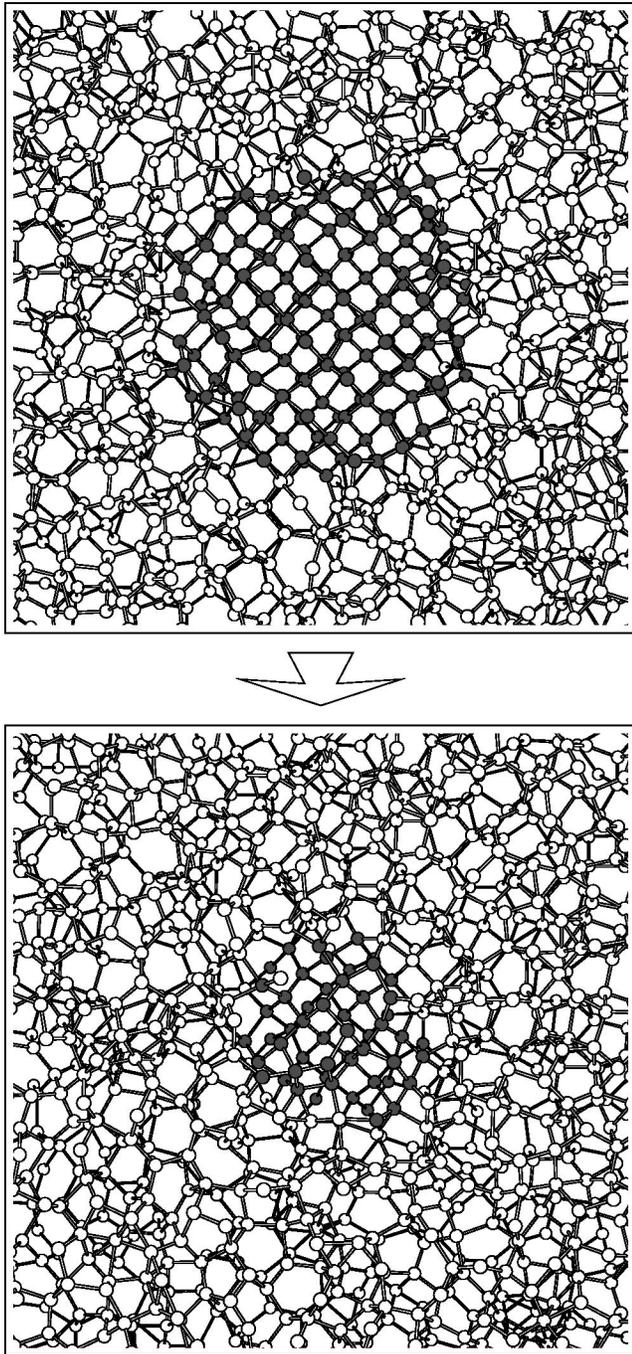
FIG. 4. Snapshots of an embedded nucleus slightly *smaller* than the critical size, at 2000 K*. The time interval between the snapshots is 0.3 ns. The size of the squares are 4.5 nm×4.5 nm.

C. Free energy on an atomic scale

By comparing Figs. 2(b) and 2(c) we note that the order as expressed by the normalized structure factor extends farther away from the center of the nucleus than does the low internal energy of the crystalline nucleus. As indicated by the vertical lines in Figs. 2(b) and 2(c) this shift is about 0.3 nm. The line in Fig. 2(b) is drawn at the position where the average internal energy is halfway between the crystalline and amorphous phase $[U = \frac{1}{2}(U_c + U_a)]$, and the line in Fig. 2(c) is drawn at the position where the normalized structure factor is one-half $[F(\mathbf{R})/F_c(\mathbf{R}) = \frac{1}{2}]$. This shift may be the origin of the interface free energy. We illustrate this by considering
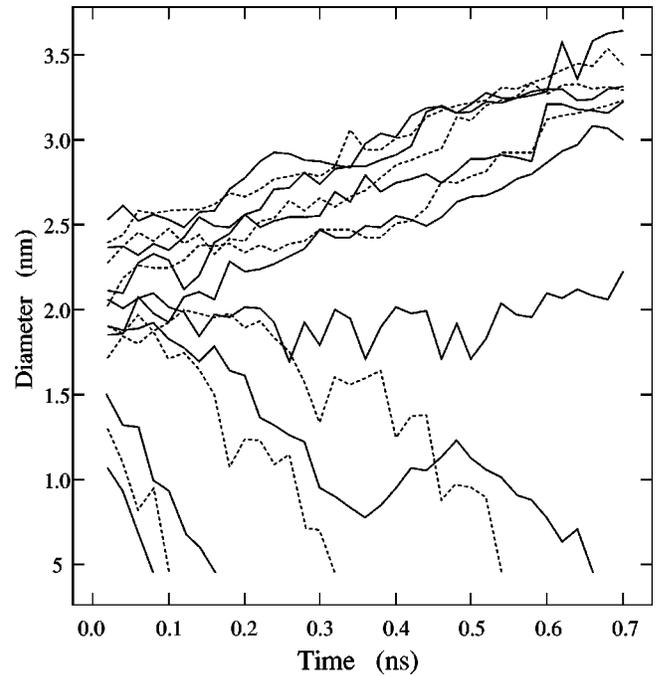

FIG. 5. Size development of the 15 nuclei at 2000 K*. This plot clearly shows the critical diameter to be about 2.0 nm. All the larger nuclei grew, while those smaller disintegrated.

Helmholtz free energy $A = U - TS$. Let us for the sake of indicating the effect of this shift assume that

$$S = k\left[1 - \frac{F(\mathbf{R})}{F_c(\mathbf{R})}\right], \tag{5}$$

where k is a constant. In Fig. 2(d) we have calculated the Helmholtz free energy for two different values of k at a certain temperature T, which effectively corresponds to two different values of temperature. We note from Fig. 2(d) that an energy barrier is formed and that the height of this barrier depends on k. The area of this barrier represents the boundary energy γ. We also see from Fig. 2(d) that with the largest k, corresponding to the largest temperature, the free energy of the amorphous matrix is only slightly higher than the free energy of the crystalline nucleus. This is what we expect at temperatures slightly below the melting temperature. Exactly at the melting temperature the energy difference should vanish.

The relationship we have proposed between the entropy and the structure factor is certainly only qualitative. Still we are confident that the shift between the vertical lines in Fig. 2(b) and 2(c) is the origin of the boundary energy γ. To make this point it is sufficient to assume that the entropy increases monotonically with decreasing structure factor.

Figures 2–4 indicate an interface that is sometimes referred to as atomically diffuse. Because silicon and germanium have strong covalent bonding, these materials usually exhibit relatively sharp, or facetted, surfaces between a solid and liquid phase.[11] Due to the smallness of the nuclei, however, we find a diffuse interface with no apparent facets on the crystals. This effect, which might lead to a surface tension depending on the size of the crystal, is observed in other simulated systems[2,7] as well as a high-resolution electron microscopy experiment.[12]

D. Evolution of the nuclei

Uttormark and Thompson[7] discussed different criteria to distinguish crystalline and liquid regions. They utilized local configuration parameters such as coordination numbers, which work well when comparing liquid and crystalline semiconductors that have distinctly different local order. However, in our case where we need to distinguish between amorphous and crystalline semiconductors these criteria are less useful. In our situation we have the choice of, for instance, using the vertical line in Figs. 2(b) and 2(c), or the maximum of the curve in Fig. 2(d). These are shifted by 0.3 nm, but for our purpose of monitoring the growth of the nuclei this is not crucial. We choose to use the vertical line in Fig. 2(c).

In Fig. 5 we have plotted the size of the 15 nuclei as a function of time. From this figure we can determine the critical size. All nuclei larger than about 2.0 nm in diameter grew, while those smaller disappeared. Notice, however, the one nucleus at 2.0 nm lingering for a long period of time. This is due to the low driving force for crystals close to the critical size. Because the small nuclei had fewer atoms, and because some of them moved slightly off center, the size determination of the small nuclei was not as accurate as it was for the larger nuclei. The relative fluctuations in the diameter for these nuclei were also larger, causing the data for small crystals to be somewhat more noisy.

Figures 3 and 4 show explicitly that a nucleus larger than the critical size grows upon annealing, while a smaller nucleus disappears. This is in agreement with classical nucleation theory. The atoms close to the boundary slowly change their configuration, joining either the central crystalline nucleus or the surrounding amorphous matrix. In the case of a subcritical nucleus, the entire nucleus will eventually be assimilated in the amorphous phase. If the nucleus is larger than the critical size, however, it will grow to fill the entire simulation cell.

From Fig. 5 we were able to calculate the velocity of the boundary as a function of the nucleus size. After averaging over all 15 nuclei, we plotted this curve in Fig. 6. From this figure we see a transition from negative growth to positive growth at about 2.0 nm. For larger nuclei the velocity seems to reach a maximum at about 0.5 m/s, while for increasingly smaller nuclei the negative velocity increases. The asymptotic velocity is in fairly good agreement with experiments[13] and other simulations on the velocity of this boundary.[14] It is, however, important to realize that because of the extremely small surface of the embedded nuclei, the growth mechanisms are somewhat different from single plane growth. All planes, and thus both lateral and kink growth, are in a way present, each with a different growth rate. We observed no twin boundaries, vacancies, or self-interstitials in the grown crystals.

IV. SUMMARY

We have studied the interface between crystalline and amorphous germanium during the nucleation and growth
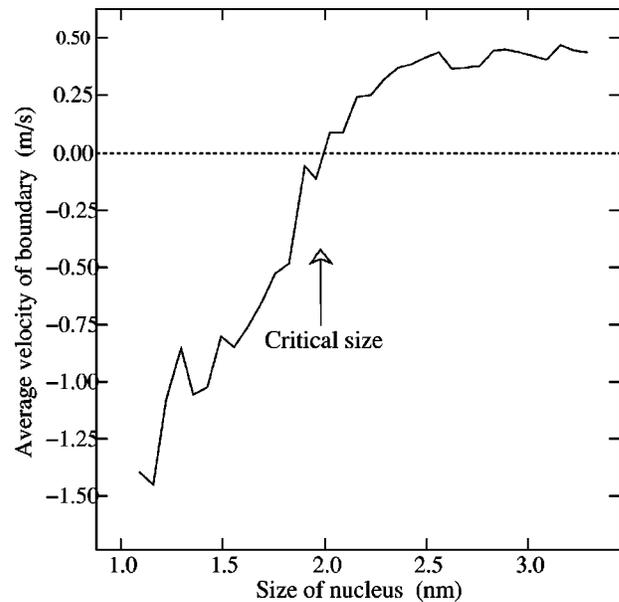
FIG. 6. Velocity of the crystalline/amorphous boundary as a function of the nuclei size simulated at 2000 K*. At about 2.0 nm the velocity is zero, while for large sizes the velocity approaches about 0.5 m/s.

process by molecular-dynamics simulations. We have shown that molecular-dynamics simulation is a powerful method to gain insight into the rearrangement taking place at the atomic level when the interface propagates. The profile of the internal energy across the interface is rather easily accessible using molecular-dynamics simulations for systems like germanium and silicon where reliable interatomic potentials are available. However, when it comes to the free energy we encounter problems because of the difficulties in extracting the entropy. We were in this study able to infer the presence of a barrier in the free energy associated with the interface tension, by realizing from the simulation that the outer atomic layer of the crystal was heavily strained. In this layer the entropy is low relative to the amorphous phase even though the internal energy is large relative to the crystal.

The fact that relevant thermodynamic properties such as entropy, and thus free energy, are not easily revealed from these simulations makes it difficult to compare our results directly with the classical macroscopic theory of nucleation. The simulations rather serve as a microscope with high spatial and temporal resolution to follow the evolution of the system at the atomic level. Based on this study of the evolution of the system we determine a critical size of the nuclei that are in good agreement with what has been derived from various experiments.[12,15–17]

[*]Email: J.K.Bording@fys.uio.no

[1] P.R. ten Wolde, M.J. Ruiz-Montero, and D. Frenkel, J. Chem. Phys. **104**, 9932 (1996).

[2] K. Yasuoka and M. Matsumoto, J. Chem. Phys. **109**, 8451 (1998).

[3] L.A. Baez and P. Clancy, J. Chem. Phys. **102**, 8138 (1995).

[4] J. Tersoff, Phys. Rev. B **38**, 9902 (1988).

[5] J. Tersoff, Phys. Rev. B **39**, 5566 (1989).

[6] F.H. Stillinger and T.A. Weber, Phys. Rev. B **31**, 5262 (1985).

[7] M.J. Uttormark, M.O. Thompson, and P. Clancy, Phys. Rev. B **47**, 15 717 (1993).

[8] J.K. Bording, Phys. Rev. B (to be published).

[9] G. Etherington, A.C. Wright, J.T. Wenzel, J.C. Dore, J.T. Clark, and R.N. Sinclair, J. Non-Cryst. Solids **48**, 265 (1982).

[10] S.K. Ma, *Statistical Mechanics* (World Scientific, Singapore, 1985).

[11] K.A. Jackson, *Kinetics of Reaction in Ionic Systems*, edited by T. J. Gray and V. D. Fre'chette (Plenum, New York, 1969), p 229.

[12] J.L. Batstone, Philos. Mag. A **67**, 51 (1993).

[13] G. Aichmayr, D. Toet, M. Mulato, P.V. Santos, A. Spangenberg, S. Christiansen, M. Albrecht, and H.P. Strunk, J. Appl. Phys. **85**, 4010 (1999).

[14] T. Motooka, Mater. Sci. Eng., A **253**, 42 (1998).

[15] H. Hofmeister, J. Dutta, and H. Hofmann, Phys. Rev. B **54**, 2856 (1996).

[16] M.H. Brodsky, *Light Scattering in Solids,* edited by M. Cardona (Springer, Berlin, 1975).

[17] R. Bisaro, J. Magariño, Y. Pastol, P. Germain, and K. Zellama, Phys. Rev. B **40**, 7655 (1989).